ACS NANO
Cite This: ACS Nano XXXX, XXX, XXX–XXX
www.acsnano.org
ARTICLE

Precision-Guided Nanospears for Targeted and High-Throughput Intracellular Gene Delivery

Xiaobin Xu,[†,‡] Shuang Hou,[†,∥] Natcha Wattanatorn,[†,‡] Fang Wang,[†,∥,△] Qing Yang,[†,‡] Chuanzhen Zhao,[†,‡] Xiao Yu,[†,∥] Hsian-Rong Tseng,[†,∥] Steven J. Jonas,*[,†,⊥,#,○] and Paul S. Weiss*[,†,‡,§]

[†]California NanoSystems Institute, University of California, Los Angeles, Los Angeles, California 90095, United States
[‡]Department of Chemistry and Biochemistry, University of California, Los Angeles, Los Angeles, California 90095, United States
[§]Department of Materials Science and Engineering, University of California, Los Angeles, Los Angeles, California 90095, United States
[∥]Department of Molecular and Medical Pharmacology, University of California, Los Angeles, Los Angeles, California 90095, United States
[⊥]Department of Pediatrics, David Geffen School of Medicine, University of California, Los Angeles, Los Angeles, California 90095, United States
[#]Eli & Edythe Broad Center of Regenerative Medicine and Stem Cell Research, University of California, Los Angeles, Los Angeles, California 90095, United States
[○]Children's Discovery and Innovation Institute, University of California, Los Angeles, Los Angeles, California 90095, United States
[△]State Key Laboratory of Molecular Engineering of Polymers and Department of Macromolecular Science, Fudan University, Shanghai 200433, China

Supporting Information

ABSTRACT: **An efficient nonviral platform for high-throughput and subcellular precision targeted intracellular delivery of nucleic acids in cell culture based on magnetic nanospears is reported. These magnetic nanospears are made of Au/Ni/Si (~5 μm in length with tip diameters <50 nm) and fabricated by nanosphere lithography and metal deposition. A magnet is used to direct the mechanical motion of a single nanospear, enabling precise control of position and three-dimensional rotation. These nanospears were further functionalized with enhanced green fluorescent protein (eGFP)-expression plasmids via a layer-by-layer approach before release from the underlying silicon substrate. Plasmid functionalized nanospears are guided magnetically to approach target adherent U87 glioblastoma cells, penetrating the cell membrane to enable intracellular delivery of the plasmid cargo. After 24 h, the target cell expresses green fluorescence indicating successful transfection. This nanospear-mediated transfection is readily scalable for the simultaneous manipulation of multiple cells using a rotating magnet. Cell viability >90% and transfection rates >80% were achieved, which exceed conventional nonviral intracellular methods. This approach is compatible with good manufacturing practices, circumventing barriers to the translation and clinical deployment of emerging cellular therapies.**

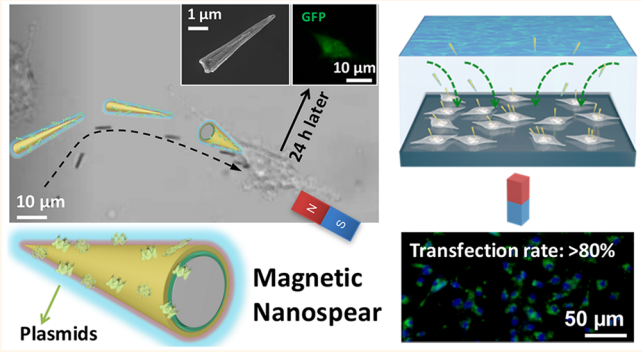

KEYWORDS: *intracellular delivery, nanosphere lithography, nanoneedle, gene delivery, drug delivery, nanorobotics, nanomotor*

High-throughput[1−3] and targeted intracellular delivery[4,5] of biomolecules is critical for applications in cell and molecular biology and emerging clinical applications that make use of gene-editing systems.[6] Existing approaches that use viruses, external electric fields, or harsh chemical reagents are either costly, apply undesirable cellular stresses or toxicities, or are inefficient. Improving the safety, speed, cost effectiveness, and efficiency of intracellular delivery methods remains a long-standing challenge.[7] Currently, membrane-disruption-based approaches are attractive as

Received: January 29, 2018
Accepted: February 26, 2018

DOI: 10.1021/acsnano.8b00763
ACS Nano XXXX, XXX, XXX–XXX

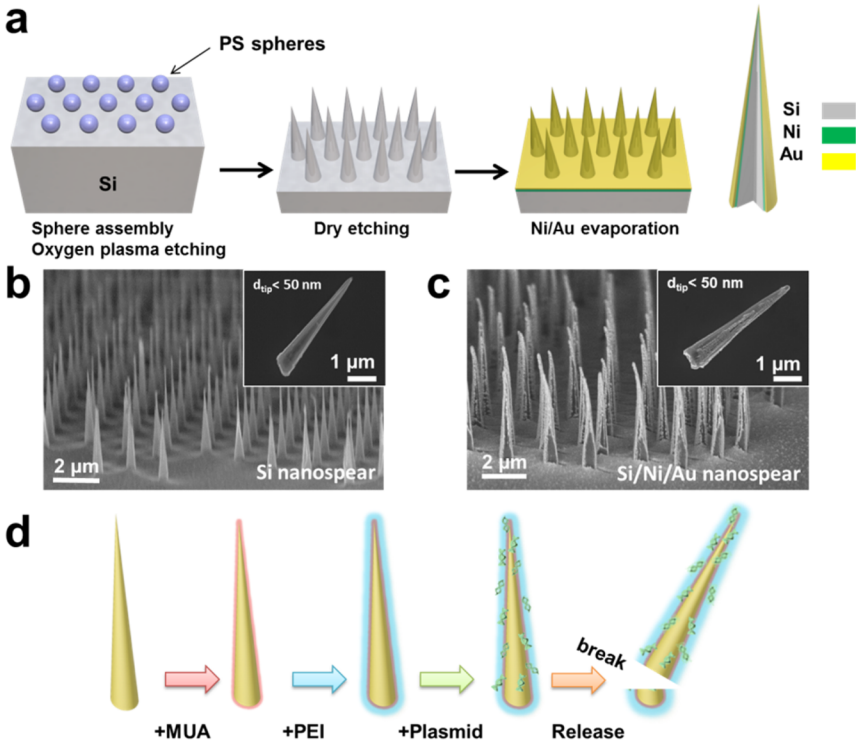

Figure 1. (a) Schematic illustrating the fabrication of magnetic nanospear arrays. Polystyrene (PS) nanospheres are first assembled on a silicon (Si) wafer followed by size reduction via oxygen plasma etching. Dry etching is then applied to etch the Si and nanospheres simultaneously to generate Si nanospear arrays. Next, layers of nickel (Ni, 40 nm) and gold (Au, 10 nm) are evaporated on the Si nanospear arrays. (b, c) Scanning electron microscopy (SEM) images of ordered nanospear arrays. Insets: individual Si and Si/Ni/Au nanospears. (d) Surface modification and release procedure of the Si/Ni/Au nanospears. 11-Mercaptoundecanoic acid (MUA) is first coated on the Si/Au/Ni nanospears; next, polyethylenimine (PEI) is electrostatically adsorbed as the second layer; negatively charged gene-modification cargo (e.g., DNA plasmid) is loaded onto the nanospear via physisorption. The functionalized Si/Ni/Au nanospears are finally released mechanically from the substrate and redispersed in deionized water.

universal delivery systems *in vitro* and *ex vivo*, including electroporation,[8] squeezing,[2,9,10] fluid shear,[7] direct microinjection,[11,12] photothermal,[13−15] sharp nanostructures,[8,11] and combinations.[2,8] In particular, configurations of needle-like nanostructures can physically penetrate flexible cell membranes to deliver biomolecules to cells efficiently and in parallel[16,17] with minimal impact on viability and metabolism due to their nanoscale sharp tips. Most reported nanoneedle platforms are comprised of arrays grown on planar substrates that support the growth of adherent cells and that can pierce cellular membranes to enable transfection.[17−19] However, difficulties with releasing the modified cells from these nanostructured substrates and collecting them for further study have precluded wider application.[16,20]

Recently, substantial progress has been made in the development of nano-/micromotor systems, which can be internally or externally powered to move in liquid environments.[4,21−38] These functional nanomaterials have been applied in biosensing,[39] biomolecule delivery,[4,23,28,30,32,40−42] and nanosurgery applications.[30] The capability for guidance and versatile cargo integration of the nano-/micromotors has enabled the active transport and delivery of therapeutic payloads.[4,30] These nanosystems have limited precision in terms of their guidance and biocompatibility due to byproducts from catalytic reactions that propel the nano-/micromotor structures to their targets.[39]

In this work, we report the rational design and fabrication of magnetic nanospears that can be configured readily for single-cell modification and that can also be scaled progressively for direct and highly efficient intracellular delivery. These biocompatible nanomaterials can be guided precisely to target cells without the need for chemical propellants via manipulation of local magnetic fields. This technique offers several advantages over conventional nonviral transfection approaches and is suitable for both molecular cell biology studies and translational medicine.

RESULTS AND DISCUSSION

The nanospears were designed and fabricated by nanosphere lithography using assembled polystyrene (PS) particles as etch templates. Nanosphere lithography is an affordable and scalable approach to generate large area periodic nanostructures such as holes, pillars, cones, needles, and wires on planar or curved substrates,[43−48] which have been broadly applied in electronics,[49] optics,[50] energy conversion/storage,[50−52] and biomedical studies.[53] The fabrication scheme of magnetic nanospears is shown in Figure 1a: polystyrene (PS) spheres (2 μm in size) self-organize into close-packed monolayers at the water/air interface then upon transfer to a silicon (Si) substrate via drop casting. The array of PS particles is then exposed to oxygen plasma to reduce the size of the spheres to ~1.4 μm. Subsequently, reactive ion etching (RIE) is applied to etch the Si substrates vertically with the PS spheres serving as a template. In this process, the PS spheres were also slowly etched while their sizes were reduced progressively to <50 nm. Silicon nanospear arrays are formed once the PS nanospheres

DOI: 10.1021/acsnano.8b00763
ACS Nano XXXX, XXX, XXX−XXX

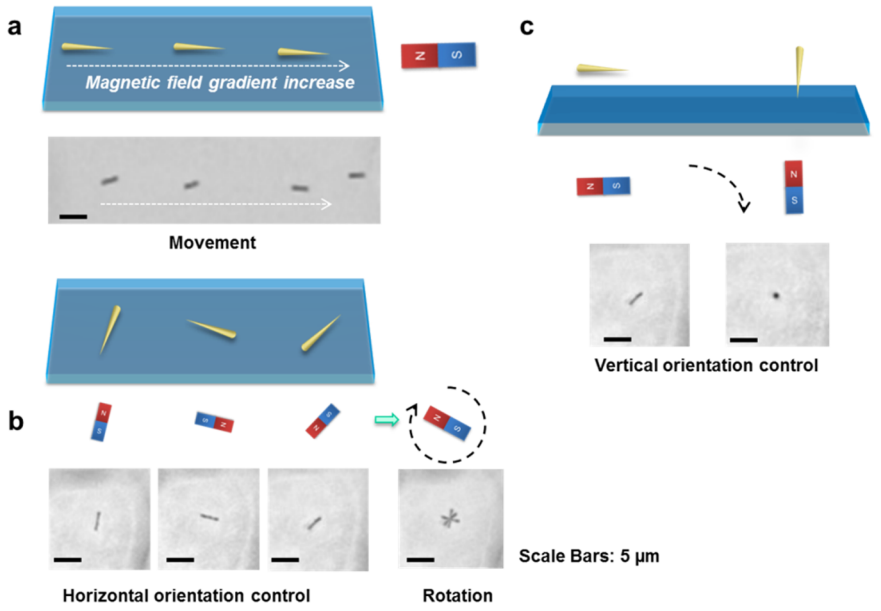

Figure 2. Schemes and experimental results of manipulation of nanospear mechanical motions using magnet a magnet including (a) movement, (b) orientation control in horizontal plane, and (c) orientation control in vertical plane.

are removed completely during the Si etching process (Figure 1b). Subsequently, nickel (Ni) and gold (Au) thin films were evaporated onto the nanospear arrays at tilted angles to preserve the sharpness of the final Au/Ni/Si nanospears as shown in Figure 1c (see methods for details). The Ni thin film is ferromagnetic, endowing the nanospears with magnetic properties,[54] while the Au layer is both biocompatible and can be tailored readily for loading biomolecules, such as loading DNA, RNA, and proteins.

Here, we use a layer-by-layer approach[55,56] to place encapsulated nucleic acid molecules on Au/Ni/Si nanospears. Alkanethiol molecules can form structurally well-defined self-assembled monolayers (SAMs) on Au to enable the conjugation of biomolecules to nanomaterials and engineered interfaces.[57−65] We used 11-mercaptoundecanoic acid (MUA) to form SAMs on the Au/Ni/Si nanospears to make the surface negatively charged. Next, a second positively charged polyethylenimine (PEI) anchoring layer is deposited onto the nanospears due to the electrostatic attractions. Negatively charged cargo molecules (*e.g.,* DNA) can be tethered to this interface. We selected enhanced green fluorescent protein (eGFP)-expression plasmids for demonstration purposes. Finally, the MUA/PEI/eGFP-expression plasmids encapsulated nanospears were released from the Si substrate via gentle mechanical scraping and redispersed in deionized water or desirable media.

These magnetic nanospears dispersed in liquid can be manipulated by a nearby small neodymium−iron−boron disk magnet. Note that it is important to control the magnetic nanospear to have their sharp tips facing the target cell. The physical orientation of each nanospear can be aligned to the orientation of the magnet to match their magnetization directions, due to the induced torque applied on the nanospear by the field of the magnet. One can magnetize the nanospears to align their tips (*e.g.*, to the south pole of a magnet) via controlled magnetization prior to removal from the silicon substrate (see Supporting Information Figure S3 for details). This phenomenon is similar to a macroscopic effect where the direction of a compass aligns to the earth's magnetic field. Nanospears can be directed to move toward the magnet if the magnetic field gradient is large enough; i.e., they are in close proximity. As a result, we can remotely manipulate the nanospears to accomplish different tasks in fluid. Our control of the direction, position, and rotation of a nanospear in three-dimensional space is illustrated in Figure 2. The magnetic-field-induced movement of nanospears is influenced by the magnetization of individual nanospears, which is defined by the mass of Ni, the magnetization of the external magnet, and their separation. Typically, the position, orientation, and speed of a nanospear can be manipulated remotely via the applied external magnetic field gradient. (1) When the magnet is positioned near to the magnetic nanospears (*e.g.*, 2−5 cm), the nanostructures align to the field of the magnet, enabling the direction of the nanospears to be controlled in three dimensions. (2) When the magnet is moved closer to the magnetic nanospears (*e.g.*, 1−2 cm), the nanospears move toward the magnet. The speed of the nanospears can be adjusted by carefully controlling the distance between the control magnet and the nanospears dispersed in solution; i.e., nanospears move faster as the control magnet is brought closer (~5 μm/s). (3) When the control magnet is moved along a desired path while kept close to the nanospears (*e.g.*, 1−2 cm), the nanostructures follow the control magnet, enabling precise directional control. Single or multiple magnetic nanospears can be manipulated remotely and simultaneously in this way using a single control magnet. If the external magnet is rotated horizontally or vertically, the nanospears rotate exactly the same way, as shown in Figure 2b.

The eGFP-expression plasmid functionalized magnetic Au/Ni/Si nanospears can be manipulated to move toward a target cell and to penetrate its cell membrane, as illustrated in Figure 3a. A typical experiment is recorded as seen in video S1 and the overlaid optical images provided in Figure 3b. After 24 h, fluorescence microscopy images indicate that the targeted cell produces green fluorescence due to the successful transfection and expression of eGFP, while the nontarget cells remain unchanged. It appears from scanning electron microscopy (SEM) images that the tip of the nanospear pierces the cell

DOI: 10.1021/acsnano.8b00763
ACS Nano XXXX, XXX, XXX−XXX

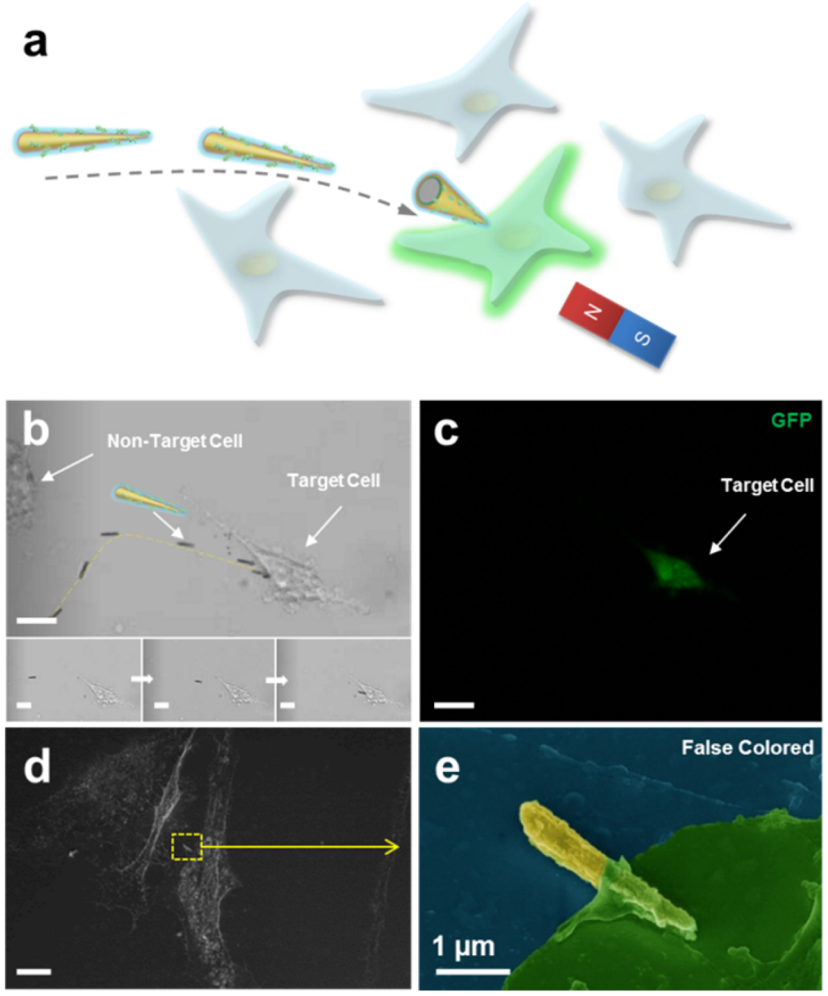

Figure 3. (a) A schematic illustration of enhanced green fluorescent protein (GFP)-expression plasmids modified Si/Ni/Au nanospear was transported and inserted into the target cell by a magnet to deliver the GFP-expression plasmid intracellularly. (b) Overlaid optical images of the process of targeted intracellular delivery and control of trajectory of a single nanospear (video provided in the Supporting Information). (c) Fluorescence microscopy image demonstrating the expression of GFP by a target U87 cell 24 h after transfection. (d) Scanning electron microscope (SEM) image illustrating a nanospear docking with its target cell. (e) At higher magnification, the nanospear is observed to insert at the plasma membrane. The SEM image is false colored to visualize the nanospear (yellow) and the cell (green). Unless noted, scale bars are 10 μm.

membrane in a manner akin to a splinter or an acupuncture needle (Figure 3d, e). This result agrees with previous findings that needle structures can physically penetrate the cytoplasmic membrane.[19] The nanospears are comprised of biocompatible materials, which are biodegraded by the target cells over time.[17] It is also possible that some nanospears are taken up by endocytosis (SEM images occasionally appear to show encapsulated nanospears, but that could also be the result of morphological changes to the cells after transfection, during sample preparation for the microscope).

Multiple magnetic nanospears can work cooperatively within a cell culture environment simultaneously to achieve robust transfection on a massive number of cells, as shown in the scheme and fluorescence microscopy images in Figure 4a–c. In a typical experiment, ~1 million nanospears dispersed in deionized water are added into a single well containing ~200,000 model U87 glioblastoma cells. A magnet is positioned concurrently along the backside of the cell culture dish and moved slowly in either a clockwise or counterclockwise direction to guide the nanospears as they travel and engage nearby cells, as shown in the bright-field optical image in Figure S2. The control of these volleys of nanospears can also be accomplished effectively by using a common magnetic stirring plate. Scanning electron micrographs of the target cells after exposure to the nanospears (Figure 4d,e) confirm that multiple nanospears are able to dock at individual cells via this approach. Taking advantage of this capability, ~80% of the target cell population is transfected with bright eGFP expression. Cell viability was quantified after transfection via acridine orange/ethidium bromide staining assays as reported elsewhere.[20] Viability tests of cells transfected by the nanospears show >90% survival with favorable proliferation potential relative to conventional methods.

Multiple nanospears may also be applied for localized transfection/delivery, which is especially important for targeting specific populations of cells in heterogeneous cultures or *in vivo*. Due to the availability of a variety of permanent magnets and reconfigurable electric magnets, one can tailor the effective size and strength of the external magnetic field applied at specific locations in order to manipulate multiple nanospears for targeted transfection. We can extend this concept further to guide the trajectory of multiple nanospears to treat cells at

DOI: 10.1021/acsnano.8b00763
ACS Nano XXXX, XXX, XXX–XXX

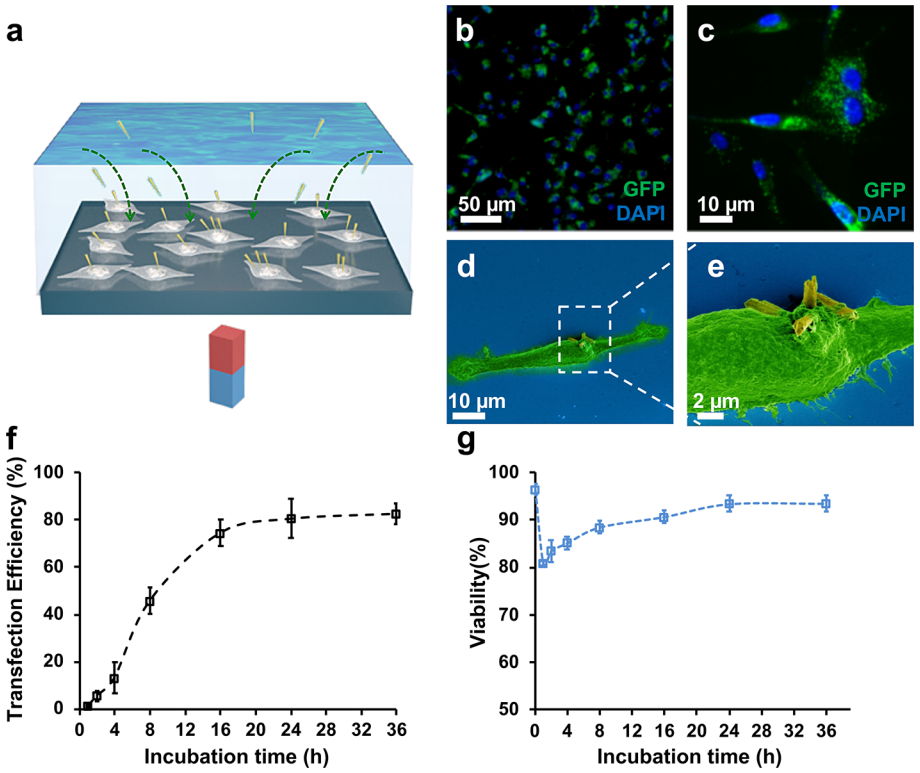

Figure 4. (a) Schematic illustrating the manipulation of multiple nanospears to achieve high-throughput transfection. (b, c) Fluorescence microscopy images of target U87 cells 24 h post transfection by green fluorescent protein (GFP)-expression plasmid containing supramolecular nanoparticles tethered to nanospears. Green: GFP. Blue: 4′,6-diamidino-2-phenylindole (DAPI). (d, e) False colored scanning electron microscopy (SEM) images illustrating multiple nanospears inserting into a target cell. (f) The transfection efficiency of based on GFP intensity versus incubation time. After 24 h, the GFP transfection efficiency is >80%. (g) Cell viability test results show the initial viability post-transfection is >80%, and over time is noted to rise as a result of cell proliferation.

different locations on the same cell culture dish. We experimentally tested this strategy by guiding nanospears carrying different expression plasmids sequentially to neighboring cells as illustrated schematically in Figure 5a. We designated specific U87 cells located at the lefthand portion of a cell culture well and selectively guided nanospears carrying eGFP-expression plasmid cargo to this area. After ∼20 min, most of the nanospears dock with their targets and are fixed at the cell membrane. The magnet is then repositioned under the righthand portion of the cell culture dish to deliver a red fluorescent protein (RFP)-expression plasmid to cells within this area. After 24 h, fluorescence microscopy images show cells on the lefthand side of the dish express green fluorescence while cells located on the right are red. A 4′,6-diamidino-2-phenylindole (DAPI) stain was used to highlight the nucleus of the cells. These experimental results demonstrate highly localized transfection as shown in Figure 5b, c. Note that the targeted positions are in close proximity in order to fit within the same field of view, which led to an observed transition region of fluorescence where cells expressed both green and red fluorescence (Figure 5d).

CONCLUSIONS AND PROSPECTS

Advances in molecular biology in the form of gene-editing tools are rapidly being used in immunology and stem cell biology. These tools will be important for the translation of emerging therapeutic strategies in immunotherapy and regenerative medicine. However, the current nonviral vector-based methods primarily used to manufacture these extraordinary gene and cellular therapies fall short at clinically relevant scales due, in part, to problematic toxicities and technical limitations resulting in low transfection efficiencies. Innovative solutions to address these challenges are approaching as nanotechnologies begin to close these gaps, enabling rapid, safe, and efficient delivery of biomolecular cargo to target cells and accelerating deployment of new medical interventions to the clinic.

Nanomotor and nanorobotics platforms possess a tantalizing versatility, which make these tools particularly well suited for applications in either the *in vitro* or *in vivo* manipulation of cell populations. Magnetically guided nanospears offer a simple, versatile, and effective platform for targeted intracellular gene delivery over large areas. A key feature is that the spears do not require a propellant for movement and positional control, avoiding potential toxicities that preclude their clinical use. While we focus on the delivery of plasmid DNA, a variety of biomolecular payloads are possible, enabling potential nanomedicine applications spanning from molecular biology to human patients. For example, this nanorobotics approach is compatible with good manufacturing practices and can be scaled easily for batch processing of large populations of cells, offering an elegant nanostructure-based solution to processing *ex vivo* harvested cells and tissues for gene-modified transplantation applications. Further optimization of autonomous guidance capabilities will provide greater precision and open potential applications for *in vivo* cell modification and gene marking. In an era where industries envision fleets of drones delivering packages to homes in the macroscopic world, guided nanostructures, such as nanospears, enable analogous solutions

DOI: 10.1021/acsnano.8b00763
ACS Nano XXXX, XXX, XXX−XXX

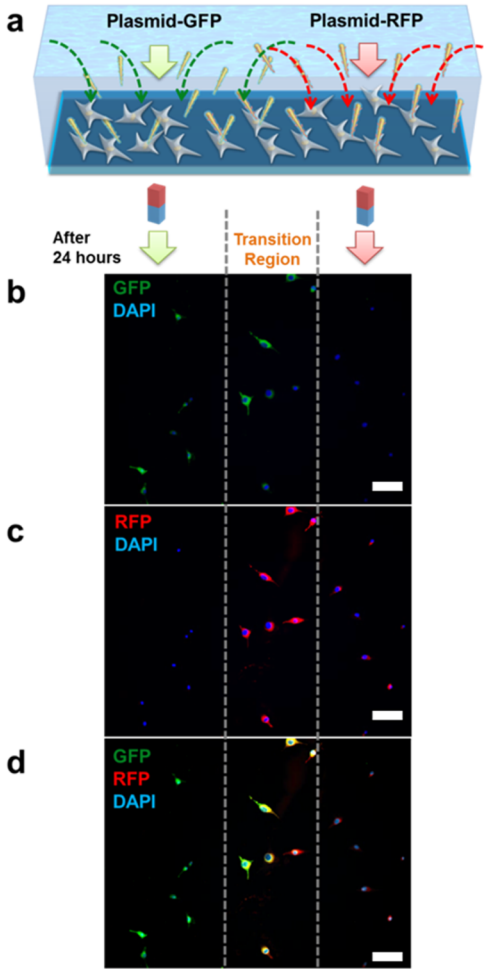

Figure 5. (a) Targeted large area cell transfection by manipulation of multiple nanospears carrying green fluorescent protein (GFP) and red fluorescent protein (RFP) respectively. (b,c) Fluorescence microscopy images after 24 h at different magnifications showing most cells have turned green. (d) Overlaid image of (b) and (c). Note that 4′,6-diamidino-2-2phenylindole (DAPI) is used to stain the nucleus of all the living and dead cells. Green: GFP. Blue: DAPI. Red: RFP. Scale bars: 50 μm.

at the cellular level. These precision manufactured nanostructures offer an effective solution to circumvent existing barriers to gene modification at large scales for the generation of cell products for gene therapy.

MATERIALS AND METHODS

Fabrication of Nanospears. Nanosphere lithography employs periodic arrays of self-assembled close-packed monolayer nanospheres as templates to pattern underlying substrate materials.[44,48] Polystyrene nanospheres (2 μm in diameter, Product No. 4202A, Thermo Fisher Scientific, MA, USA) were assembled into close-packed monolayers on a 2 cm × 2 cm or larger Si substrate as reported elsewhere.[43,46] Oxygen plasma (Oxford Plasmalab 80 Plus, Oxford Instruments, Abingdon, UK) with 35 sccm of O_2 and 10 sccm of Ar at a pressure of 60 mTorr and radio frequency (RF) power of 60 W for 10 min was applied to reduce the size of PS nanospheres to ∼1.4 μm. To achieve sharp Si needles with high aspect ratios, single-step RIE of Si was completed in a simultaneous flow of 20 sccm C_4F_8, 27 sccm SF_6, and 5 sccm Ar with the inductively coupled plasma (ICP) power of 650 W for 7 min (STS AOE Advanced Oxide Etcher). The SF_6 was used to etch the unprotected areas, and the C_4F_8 was used to deposit fluorinated polymer to protect the side walls of the etched structures.

Fabrication of Magnetic Au/Ni/Si Nanospears. The nanoneedle substrates were loaded into the vacuum chamber of an electron beam metal evaporator (Kurt J. Lesker Company, Jefferson Hills, PA) and held at a base pressure of ∼1×10^{-7} Torr. The substrates were mounted with fixed positions and orientations within the chamber such that their surface normal was inclined at an angle of 20° away from the metal source. A film of 100 nm Ni was deposited at a rate of ∼1 Å/s. Then, 40 nm Au films were deposited at an angle of 20° and −20° at a rate of ∼0.5 Å/s.

Surface Modification of the Magnetic Au/Ni/Si Nanospears. A three-step layer-by-layer approach through electrostatic interaction is used to coat the Au/Ni/Si nanospears with desired cargo. Step 1: The Au/Ni/Si nanospear substrate is immersed into a 11-mercapto-undecanoic acid solution (MUA, 1 mM in ethanol) for ∼30 min to form MUA SAMs on Au/Ni/Si nanospears via gold−thiolate bonds, then rinsed with ethanol, and blow-dried with N_2 gas several times to remove excessive thiol molecules. Step 2: the substrate is immersed in 1 wt % poly(ethylenimine) (PEI, Sigma-Aldrich) solution for ∼30 min and then washed with water. Step 3, the substrate is immersed in ∼2 mL water with 2.0 μg of the desired expression plasmid and incubated overnight. Then, the substrate is rinsed in deionized water and dried. The plasmid-coated Au/Ni/Si nanospears (∼10 million) are carefully released from the Si substrate (0.5 cm^2) via mechanical scraping with a razor blade and then redispersed in ∼2 mL water to reach a nanospear density of ∼5×10^6 mL^{-1}. Finally, ultrasound is used to reduce aggregation of the magnetic nanospears.

Targeted Single Cell Intracellular Gene Delivery. For gene delivery to individual cells, the stock nanospear solution is further diluted at least ∼20×. U87 cells are precultured on a glass slide, which is mounted on the stage of an inverted optical microscope. In a typical experiment, 10 μL of diluted nanospear solution are added to the cell culture medium. After ∼1−2 min, nanospears precipitate to the bottom of the cell culture medium. A cylindrical neodymium−iron−boron magnet (diameter, 10 mm; length, 9 mm) with a magnetic field intensity of ∼0.5 T measured from its surface is used to direct the mechanical motion of the nanospheres within the cell culture environment. The motion of individual nanospears can be observed with an optical microscope (40×) as the magnet is moved into proximity with the nanospears. When the magnet−nanospear separation is ∼5 cm, the nanospears align in the direction of the magnetic field. When the magnet is moved closer (<2 cm), the increased magnetic field gradient attracts the nanospears to move toward the magnet, enabling control of both the direction and speed of motion of each nanospear. After docking a nanospear to its target cell, the magnet is held in position for ∼5 min to ensure that the nanospear is securely tethered to the cell. Expression of reporter fluorescent proteins from nanospear-treated cells was monitored by fluorescence microscopy.

High-Throughput Intracellular Gene Delivery. A suspension containing ∼1 million nanospears carrying eGFP expression-plasmid cargo was added into a well of a 6-well disposable tissue culture plate containing ∼200,000 U87 cells. A small magnet was next positioned under the culture plate and moved back-and-forth for ∼10 min to distribute the nanospears throughout the entire cell culture area and to ensure that the nanospears engage stably with the target cell population. Cells treated with eGFP-nanospears were monitored for fluorescence expression after 24 h.

ASSOCIATED CONTENT

Supporting Information

The Supporting Information is available free of charge on the ACS Publications website at DOI: 10.1021/acsnano.8b00763.

Figures S1, S2, S3: scanning electron micrographs of self-assembled nanospheres; bright field and fluorescence optical micrographs of transfection of large numbers of cells by multiple nanospears; magnetization of the nanospears and identification of the direction/orientation of nanospears' tips by optical microscopy (PDF)

DOI: 10.1021/acsnano.8b00763
ACS Nano XXXX, XXX, XXX−XXX

Video S1: Magnetic manipulation of a single nanospear for targeted single-cell transfection (AVI)

AUTHOR INFORMATION

Corresponding Authors

*E-mail: sjjonas@mednet.ucla.edu.

*E-mail: psw@cnsi.ucla.edu.

ORCID

Xiaobin Xu: 0000-0002-3479-0130

Shuang Hou: 0000-0001-5487-2427

Qing Yang: 0000-0003-4422-5300

Chuanzhen Zhao: 0000-0003-0162-1231

Hsian-Rong Tseng: 0000-0001-9028-8527

Steven J. Jonas: 0000-0002-8111-0249

Paul S. Weiss: 0000-0001-5527-6248

Author Contributions

All authors conceived of and designed the experiments. The nanostructures were fabricated by X.X., N.W., Q.Y., and C.Z.; the nanomanipulation experiments were performed by X.X. and H.S.; and the transfection and viability assays were performed by H.S., F.W., and X.Y. The data were analyzed by X.X., H.S, N.W., F.W., Q.Y., H.R.T., and S.J.

Notes

The authors declare no competing financial interest.

ACKNOWLEDGMENTS

We gratefully acknowledge support from the National Science Foundation Grant #CMMI-1636136. H.R.T. thanks the support from National Institutes of Health Grant #R21EB016270. S.J.J. acknowledges the support of the Eli and Edythe Broad Center of Regenerative Medicine and Stem Cell Research at UCLA Training Program through its Clinical Fellowship Training Award Program as well as Young Investigator Award funds from the Hyundai Hope on Wheels Foundation and the Alex's Lemonade Stand Foundation for Pediatric Cancer Research. P.S.W. and S.J.J. acknowledge a UCLA David Geffen School of Medicine Regenerative Medicine Theme Award and Eli and Edythe Broad Center of Regenerative Medicine and Stem Cell Research at UCLA for seed funding. F.W. thanks the support from the National Science Foundation of China Grant #51603042. C.Z. thanks the China Scholarship Council for the CSC-UCLA scholarship. N.W. thanks the Royal Thai Government for the graduate fellowship. We also acknowledge the facilities and thank the staff of the Electron Imaging Center, Integrated Systems Nanofabrication Cleanroom of the California NanoSystems Institute, and NanoLab. We thank Jerome Bixby, Harry Kleiner, Otto Klement, and Leonard Rosenman for inspiration.

REFERENCES

(1) Wang, S.; Liu, K.; Liu, J.; Yu, Z. T. F.; Xu, X.; Zhao, L.; Lee, T.; Lee, E. K.; Reiss, J.; Lee, Y.-K.; Chung, L. W. K.; Huang, J.; Rettig, M.; Seligson, D.; Duraiswamy, K. N.; Shen, C. K. F.; Tseng, H.-R. Highly Efficient Capture of Circulating Tumor Cells by Using Nanostructured Silicon Substrates with Integrated Chaotic Micromixers. *Angew. Chem., Int. Ed.* **2011**, *50*, 3084−3088.

(2) Ding, X.; Stewart, M. P.; Sharei, A.; Weaver, J. C.; Langer, R. S.; Jensen, K. F. High-Throughput Nuclear Delivery and Rapid Expression of DNA *via* Mechanical and Electrical Cell-Membrane Disruption. *Nat. Biomed. Eng.* **2017**, *1*, 0039.

(3) Zhang, F.; Jiang, Y.; Liu, X.; Meng, J.; Zhang, P.; Liu, H.; Yang, G.; Li, G.; Jiang, L.; Wan, L.-J.; Hu, J.-S.; Wang, S. Hierarchical Nanowire Arrays as Three-Dimensional Fractal Nanobiointerfaces for High Efficient Capture of Cancer Cells. *Nano Lett.* **2016**, *16*, 766−772.

(4) Fan, D.; Yin, Z.; Cheong, R.; Zhu, F. Q.; Cammarata, R. C.; Chien, C. L.; Levchenko, A. Subcellular-Resolution Delivery of a Cytokine through Precisely Manipulated Nanowires. *Nat. Nanotechnol.* **2010**, *5*, 545−551.

(5) García-López, V.; Chen, F.; Nilewski, L. G.; Duret, G.; Aliyan, A.; Kolomeisky, A. B.; Robinson, J. T.; Wang, G.; Pal, R.; Tour, J. M. Molecular Machines Open Cell Membranes. *Nature* **2017**, *548*, 567−572.

(6) Whitehead, K. A.; Langer, R.; Anderson, D. G. Knocking Down Barriers: Advances in siRNA Delivery. *Nat. Rev. Drug Discovery* **2009**, *8*, 129−138.

(7) Stewart, M. P.; Sharei, A.; Ding, X.; Sahay, G.; Langer, R.; Jensen, K. F. *In Vitro* and *Ex Vivo* Strategies for Intracellular Delivery. *Nature* **2016**, *538*, 183−192.

(8) Xie, X.; Xu, A. M.; Leal-Ortiz, S.; Cao, Y.; Garner, C. C.; Melosh, N. A. Nanostraw−Electroporation System for Highly Efficient Intracellular Delivery and Transfection. *ACS Nano* **2013**, *7*, 4351−4358.

(9) Lee, J.; Sharei, A.; Sim, W. Y.; Adamo, A.; Langer, R.; Jensen, K. F.; Bawendi, M. G. Nonendocytic Delivery of Functional Engineered Nanoparticles into the Cytoplasm of Live Cells Using a Novel, High-Throughput Microfluidic Device. *Nano Lett.* **2012**, *12*, 6322−6327.

(10) Kollmannsperger, A.; Sharei, A.; Raulf, A.; Heilemann, M.; Langer, R.; Jensen, K. F.; Wieneke, R.; Tampé, R. Live-Cell Protein Labelling with Nanometre Precision by Cell Squeezing. *Nat. Commun.* **2016**, *7*, 10372.

(11) Yoo, S. M.; Kang, M.; Kang, T.; Kim, D. M.; Lee, S. Y.; Kim, B. Electrotriggered, Spatioselective, Quantitative Gene Delivery into a Single Cell Nucleus by Au Nanowire Nanoinjector. *Nano Lett.* **2013**, *13*, 2431−2435.

(12) Bruckbauer, A.; Ying, L.; Rothery, A. M.; Zhou, D.; Shevchuk, A. I.; Abell, C.; Korchev, Y. E.; Klenerman, D. Writing with DNA and Protein Using a Nanopipet for Controlled Delivery. *J. Am. Chem. Soc.* **2002**, *124*, 8810−8811.

(13) Tirlapur, U. K.; König, K. Cell Biology: Targeted Transfection by Femtosecond Laser. *Nature* **2002**, *418*, 290−291.

(14) Wu, Y.-C.; Wu, T.-H.; Clemens, D. L.; Lee, B.-Y.; Wen, X.; Horwitz, M. A.; Teitell, M. A.; Chiou, P.-Y. Massively Parallel Delivery of Large Cargo into Mammalian Cells with Light Pulses. *Nat. Methods* **2015**, *12*, 439−444.

(15) Wu, T. H.; Sagullo, E.; Case, D.; Zheng, X.; Li, Y.; Hong, J. S.; TeSlaa, T.; Patananan, A. N.; McCaffery, J. M.; Niazi, K.; Braas, D.; Koehler, C. M.; Graeber, T. G.; Chiou, P. Y.; Teitell, M. A. Mitochondrial Transfer by Photothermal Nanoblade Restores Metabolite Profile in Mammalian Cells. *Cell Metab.* **2016**, *23*, 921−929.

(16) Peng, J.; Garcia, M. A.; Choi, J.-s.; Zhao, L.; Chen, K.-J.; Bernstein, J. R.; Peyda, P.; Hsiao, Y.-S.; Liu, K. W.; Lin, W.-Y.; Pyle, A. D.; Wang, H.; Hou, S.; Tseng, H.-R. Molecular Recognition Enables Nanosubstrate-Mediated Delivery of Gene-Encapsulated Nanoparticles with High Efficiency. *ACS Nano* **2014**, *8*, 4621−4629.

(17) Chiappini, C.; De Rosa, E.; Martinez, J. O.; Liu, X.; Steele, J.; Stevens, M. M.; Tasciotti, E. Biodegradable Silicon Nanoneedles Delivering Nucleic Acids Intracellularly Induce Localized *in Vivo* neovascularization. *Nat. Mater.* **2015**, *14*, 532−539.

(18) Elnathan, R.; Delalat, B.; Brodoceanu, D.; Alhmoud, H.; Harding, F. J.; Buehler, K.; Nelson, A.; Isa, L.; Kraus, T.; Voelcker, N. H. Maximizing Transfection Efficiency of Vertically Aligned Silicon Nanowire Arrays. *Adv. Funct. Mater.* **2015**, *25*, 7215−7225.

(19) Chiappini, C.; Martinez, J. O.; De Rosa, E.; Almeida, C. S.; Tasciotti, E.; Stevens, M. M. Biodegradable Nanoneedles for Localized Delivery of Nanoparticles *in Vivo*: Exploring the Biointerface. *ACS Nano* **2015**, *9*, 5500−5509.

(20) Hou, S.; Choi, J.-s.; Chen, K.-J.; Zhang, Y.; Peng, J.; Garcia, M. A.; Yu, J.-H.; Thakore-Shah, K.; Ro, T.; Chen, J.-F.; Peyda, P.; Fan, G.; Pyle, A. D.; Wang, H.; Tseng, H.-R. Supramolecular Nanosubstrate-

DOI: 10.1021/acsnano.8b00763
ACS Nano XXXX, XXX, XXX−XXX

Mediated Delivery for Reprogramming and Transdifferentiation of Mammalian Cells. *Small* **2015**, *11*, 2499−2504.
(21) Paxton, W. F.; Kistler, K. C.; Olmeda, C. C.; Sen, A.; St. Angelo, S. K.; Cao, Y.; Mallouk, T. E.; Lammert, P. E.; Crespi, V. H. Catalytic Nanomotors: Autonomous Movement of Striped Nanorods. *J. Am. Chem. Soc.* **2004**, *126*, 13424−13431.
(22) Kline, T. R.; Paxton, W. F.; Mallouk, T. E.; Sen, A. Catalytic Nanomotors: Remote-Controlled Autonomous Movement of Striped Metallic Nanorods. *Angew. Chem.* **2005**, *117*, 754−756.
(23) Baraban, L.; Makarov, D.; Streubel, R.; Mönch, I.; Grimm, D.; Sanchez, S.; Schmidt, O. G. Catalytic Janus Motors on Microfluidic Chip: Deterministic Motion for Targeted Cargo Delivery. *ACS Nano* **2012**, *6*, 3383−3389.
(24) Kim, K.; Xu, X.; Guo, J.; Fan, D. L. Ultrahigh-Speed Rotating Nanoelectromechanical System Devices Assembled from Nanoscale Building Blocks. *Nat. Commun.* **2014**, *5*, 3632.
(25) Xu, X.; Liu, C.; Kim, K.; Fan, D. L. Electric-Driven Rotation of Silicon Nanowires and Silicon Nanowire Motors. *Adv. Funct. Mater.* **2014**, *24*, 4843−4850.
(26) Kim, K.; Guo, J.; Xu, X.; Fan, D. Micromotors with Step-Motor Characteristics by Controlled Magnetic Interactions among Assembled Components. *ACS Nano* **2015**, *9*, 548−554.
(27) Xu, X.; Kim, K.; Fan, D. Tunable Release of Multiplex Biochemicals by Plasmonically Active Rotary Nanomotors. *Angew. Chem., Int. Ed.* **2015**, *54*, 2525−2529.
(28) Esteban-Fernández de Ávila, B.; Angell, C.; Soto, F.; Lopez-Ramirez, M. A.; Báez, D. F.; Xie, S.; Wang, J.; Chen, Y. Acoustically Propelled Nanomotors for Intracellular siRNA Delivery. *ACS Nano* **2016**, *10*, 4997−5005.
(29) Dong, R.; Zhang, Q.; Gao, W.; Pei, A.; Ren, B. Highly Efficient Light-Driven TiO_2−Au Janus Micromotors. *ACS Nano* **2016**, *10*, 839−844.
(30) Li, J.; Esteban-Fernández de Ávila, B.; Gao, W.; Zhang, L.; Wang, J. Micro/Nanorobots for Biomedicine: Delivery, Surgery, Sensing, and Detoxification. *Science Robotics* **2017**, *2*, eaam6431.
(31) Li, T.; Li, J.; Morozov, K. I.; Wu, Z.; Xu, T.; Rozen, I.; Leshansky, A. M.; Li, L.; Wang, J. Highly Efficient Freestyle Magnetic Nanoswimmer. *Nano Lett.* **2017**, *17*, 5092−5098.
(32) Esteban-Fernández de Ávila, B.; Ramírez-Herrera, D. E.; Campuzano, S.; Angsantikul, P.; Zhang, L.; Wang, J. Nanomotor-Enabled pH-Responsive Intracellular Delivery of Caspase-3: Toward Rapid Cell Apoptosis. *ACS Nano* **2017**, *11*, 5367−5374.
(33) Xu, L.; Mou, F.; Gong, H.; Luo, M.; Guan, J. Light-Driven Micro/Nanomotors: From Fundamentals to Applications. *Chem. Soc. Rev.* **2017**, *46*, 6905−6926.
(34) Magdanz, V.; Medina-Sánchez, M.; Schwarz, L.; Xu, H.; Elgeti, J.; Schmidt, O. G. Spermatozoa as Functional Components of Robotic Microswimmers. *Adv. Mater.* **2017**, *29*, 1606301.
(35) Ren, L.; Zhou, D.; Mao, Z.; Xu, P.; Huang, T. J.; Mallouk, T. E. Rheotaxis of Bimetallic Micromotors Driven by Chemical−Acoustic Hybrid Power. *ACS Nano* **2017**, *11*, 10591−10598.
(36) Wang, H.; Potroz, M. G.; Jackman, J. A.; Khezri, B.; Marić, T.; Cho, N.-J.; Pumera, M. Bioinspired Spiky Micromotors Based on Sporopollenin Exine Capsules. *Adv. Funct. Mater.* **2017**, *27*, 1702338.
(37) Guo, J.; Gallegos, J. J.; Tom, A. R.; Fan, D. Electric-Field Guided Precision Manipulation of Catalytic Nanomotors for Cargo Delivery and Powering Nanoelectromechanical Devices. *ACS Nano* **2018**, in press. DOI: 10.1021/acsnano.7b06824.
(38) Li, J.; Liu, W.; Wang, J.; Rozen, I.; He, S.; Chen, C.; Kim, H. G.; Lee, H.-J.; Lee, H.-B.-R.; Kwon, S.-H.; Li, T.; Li, L.; Wang, J.; Mei, Y. Nanoconfined Atomic Layer Deposition of TiO_2/Pt Nanotubes: Toward Ultrasmall Highly Efficient Catalytic Nanorockets. *Adv. Funct. Mater.* **2017**, *27*, 1700598.
(39) Xu, X.; Li, H.; Hasan, D.; Ruoff, R. S.; Wang, A. X.; Fan, D. L. Near-Field Enhanced Plasmonic-Magnetic Bifunctional Nanotubes for Single Cell Bioanalysis. *Adv. Funct. Mater.* **2013**, *23*, 4332−4338.
(40) Hasani-Sadrabadi, M. M.; Majedi, F. S.; Bensinger, S. J.; Wu, B. M.; Bouchard, L.-S.; Weiss, P. S.; Moshaverinia, A. Mechanobiological Mimickry of Helper T Lymphocytes to Evaluate Cell-Biomaterials Crosstalk. *Adv. Mater.* **2018**, in press DOI: 10.1002/adma.201706780.
(41) Xu, H.; Medina-Sánchez, M.; Magdanz, V.; Schwarz, L.; Hebenstreit, F.; Schmidt, O. G. Sperm-Hybrid Micromotor for Targeted Drug Delivery. *ACS Nano* **2018**, *12*, 327−337.
(42) Pelaz, B.; Alexiou, C.; Alvarez-Puebla, R. A.; Alves, F.; Andrews, A. M.; Ashraf, S.; Balogh, L. P.; Ballerini, L.; Bestetti, A.; Brendel, C.; Bosi, S.; Carril, M.; Chan, W. C. W.; Chen, C.; Chen, X.; Chen, X.; Cheng, Z.; Cui, D.; Du, J.; Dullin, C.; et al. Diverse Applications of Nanomedicine. *ACS Nano* **2017**, *11*, 2313−2381.
(43) Hulteen, J. C.; Van Duyne, R. P. Nanosphere Lithography: A Materials General Fabrication Process for Periodic Particle Array Surfaces. *J. Vac. Sci. Technol., A* **1995**, *13*, 1553−1558.
(44) Haynes, C. L.; Van Duyne, R. P. Nanosphere Lithography: A Versatile Nanofabrication Tool for Studies of Size-Dependent Nanoparticle Optics. *J. Phys. Chem. B* **2001**, *105*, 5599−5611.
(45) Wang, X. D.; Graugnard, E.; King, J. S.; Wang, Z. L.; Summers, C. J. Large-Scale Fabrication of Ordered Nanobowl Arrays. *Nano Lett.* **2004**, *4*, 2223−2226.
(46) Chen, K.; Rajeeva, B. B.; Wu, Z.; Rukavina, M.; Dao, T. D.; Ishii, S.; Aono, M.; Nagao, T.; Zheng, Y. Moiré Nanosphere Lithography. *ACS Nano* **2015**, *9*, 6031−6040.
(47) Gao, P. Q.; He, J.; Zhou, S. Q.; Yang, X.; Li, S. Z.; Sheng, J.; Wang, D.; Yu, T. B.; Ye, J. C.; Cui, Y. Large-Area Nanosphere Self-Assembly by a Micro-Propulsive Injection Method for High Throughput Periodic Surface Nanotexturing. *Nano Lett.* **2015**, *15*, 4591−4598.
(48) Xu, X.; Yang, Q.; Wattanatorn, N.; Zhao, C.; Chiang, N.; Jonas, S. J.; Weiss, P. S. Multiple-Patterning Nanosphere Lithography for Fabricating Periodic Three-Dimensional Hierarchical Nanostructures. *ACS Nano* **2017**, *11*, 10384−10391.
(49) Zhang, L.; Zhong, X.; Pavlica, E.; Li, S.; Klekachev, A.; Bratina, G.; Ebbesen, T. W.; Orgiu, E.; Samorì, P. A Nanomesh Scaffold for Supramolecular Nanowire Optoelectronic Devices. *Nat. Nanotechnol.* **2016**, *11*, 900−906.
(50) Garnett, E.; Yang, P. Light Trapping in Silicon Nanowire Solar Cells. *Nano Lett.* **2010**, *10*, 1082−1087.
(51) Kelzenberg, M. D.; Boettcher, S. W.; Petykiewicz, J. A.; Turner-Evans, D. B.; Putnam, M. C.; Warren, E. L.; Spurgeon, J. M.; Briggs, R. M.; Lewis, N. S.; Atwater, H. A. Enhanced Absorption and Carrier Collection in Si Wire Arrays for Photovoltaic Applications. *Nat. Mater.* **2010**, *9*, 239−244.
(52) Kim, Y. Y.; Kim, H. J.; Jeong, J. H.; Lee, J.; Choi, J. H.; Jung, J. Y.; Lee, J. H.; Cheng, H.; Lee, K. W.; Choi, D. G. Facile Fabrication of Silicon Nanotube Arrays and Their Application in Lithium-Ion Batteries. *Adv. Eng. Mater.* **2016**, *18*, 1349−1353.
(53) Bucaro, M. A.; Vasquez, Y.; Hatton, B. D.; Aizenberg, J. Fine-Tuning the Degree of Stem Cell Polarization and Alignment on Ordered Arrays of High-Aspect-Ratio Nanopillars. *ACS Nano* **2012**, *6*, 6222−6230.
(54) Xu, X.; Kim, K.; Li, H.; Fan, D. L. Ordered Arrays of Raman Nanosensors for Ultrasensitive and Location Predictable Biochemical Detection. *Adv. Mater.* **2012**, *24*, 5457−5463.
(55) Elbakry, A.; Zaky, A.; Liebl, R.; Rachel, R.; Goepferich, A.; Breunig, M. Layer-by-Layer Assembled Gold Nanoparticles for siRNA Delivery. *Nano Lett.* **2009**, *9*, 2059−2064.
(56) Richardson, J. J.; Bjornmalm, M.; Caruso, F. Technology-Driven Layer-by-Layer Assembly of Nanofilms. *Science* **2015**, *348*, aaa2491.
(57) Chaki, N. K.; Vijayamohanan, K. Self-Assembled Monolayers as a Tunable Platform for Biosensor Applications. *Biosens. Bioelectron.* **2002**, *17*, 1−12.
(58) Smith, R. K.; Lewis, P. A.; Weiss, P. S. Patterning Self-Assembled Monolayers. *Prog. Surf. Sci.* **2004**, *75*, 1−68.
(59) Love, J. C.; Estroff, L. A.; Kriebel, J. K.; Nuzzo, R. G.; Whitesides, G. M. Self-Assembled Monolayers of Thiolates on Metals as a Form of Nanotechnology. *Chem. Rev.* **2005**, *105*, 1103−1170.
(60) Cao, H. H.; Nakatsuka, N.; Serino, A. C.; Liao, W. S.; Cheunkar, S.; Yang, H.; Weiss, P. S.; Andrews, A. M. Controlled DNA Patterning

DOI: 10.1021/acsnano.8b00763
ACS Nano XXXX, XXX, XXX−XXX

by Chemical Lift-Off Lithography: Matrix Matters. *ACS Nano* **2015**, *9*, 11439−11454.
(61) Liao, W.-S.; Cheunkar, S.; Cao, H. H.; Bednar, H. R.; Weiss, P. S.; Andrews, A. M. Subtractive Patterning *via* Chemical Lift-Off Lithography. *Science* **2012**, *337*, 1517−1521.
(62) Cheng, X.; Lowe, S. B.; Reece, P. J.; Gooding, J. J. Colloidal Silicon Quantum Dots: From Preparation to the Modification of Self-Assembled Monolayers (SAMs) for Bio-Applications. *Chem. Soc. Rev.* **2014**, *43*, 2680−2700.
(63) Cao, H. H.; Nakatsuka, N.; Liao, W.-S.; Serino, A. C.; Cheunkar, S.; Yang, H.; Weiss, P. S.; Andrews, A. M. Advancing Biocapture Substrates *via* Chemical Lift-Off Lithography. *Chem. Mater.* **2017**, *29*, 6829−6839.
(64) Andrews, A. M.; Liao, W.-S.; Weiss, P. S. Double-Sided Opportunities Using Chemical Lift-Off Lithography. *Acc. Chem. Res.* **2016**, *49*, 1449−1457.
(65) Xu, X.; Yang, Q.; Cheung, K. M.; Zhao, C.; Wattanatorn, N.; Belling, J. N.; Abendroth, J. M.; Slaughter, L. S.; Mirkin, C. A.; Andrews, A. M.; Weiss, P. S. Polymer-Pen Chemical Lift-Off Lithography. *Nano Lett.* **2017**, *17*, 3302−3311.

DOI: 10.1021/acsnano.8b00763
ACS Nano XXXX, XXX, XXX−XXX